

# Fluorescence Lifetime Measurement of Prefibrillar Sick Cell Hemoglobin Oligomers as a Platform for Drug Discovery in Sick Cell Disease

Nagamani Vunnam, Scott Hansen, Dillon C. Williams, MaryJane Olivia Been, Chih Hung Lo, Anil K. Pandey, Carolyn N. Paulson, John A. Rohde, David D. Thomas, Jonathan N. Sachs,\* and David K. Wood\*



Cite This: *Biomacromolecules* 2022, 23, 3822–3830



Read Online

ACCESS |



Metrics & More

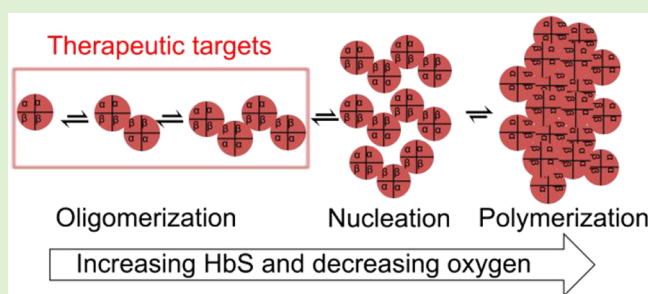


Article Recommendations



Supporting Information

**ABSTRACT:** The molecular origin of sickle cell disease (SCD) has been known since 1949, but treatments remain limited. We present the first high-throughput screening (HTS) platform for discovering small molecules that directly inhibit sickle hemoglobin (HbS) oligomerization and improve blood flow, potentially overcoming a long-standing bottleneck in SCD drug discovery. We show that at concentrations far below the threshold for nucleation and rapid polymerization, deoxygenated HbS forms small assemblies of multiple  $\alpha_2\beta_2$  tetramers. Our HTS platform leverages high-sensitivity fluorescence lifetime measurements that monitor these temporally stable prefibrillar HbS oligomers. We show that this approach is sensitive to compounds that inhibit HbS polymerization with or without modulating hemoglobin oxygen binding affinity. We also report the results of a pilot small-molecule screen in which we discovered and validated several novel inhibitors of HbS oligomerization.



## INTRODUCTION

Sickle cell disease (SCD) is a devastating hereditary disorder that afflicts tens of millions worldwide, contributing to shortened lifespan, high infant mortality rates, and significantly reduced quality of life. Despite the severe health need, treatment options for SCD are limited to four FDA-approved therapies: voxelotor, crizanlizumab-tmca, L-glutamine, and hydroxyurea. Out of these four drugs, only voxelotor directly binds to hemoglobin and prevents sickle hemoglobin (HbS) polymerization by increasing hemoglobin's affinity for oxygen and stabilizing the oxy-hemoglobin state.<sup>1,2</sup> L-Glutamine reduces oxidative damage to red blood cells by improving the redox potential of nicotinamide adenine dinucleotide,<sup>3</sup> and crizanlizumab-tmca binds to P-selectin and blocks interactions between endothelial cells, platelets, red blood cells, and leukocytes.<sup>4</sup> Hydroxyurea upregulates fetal hemoglobin, which can inhibit HbS polymerization.<sup>5,6</sup> Notably, two of these treatments were existing molecules for other indications and none of the 4 has been demonstrated clinically as a potent therapy that dramatically improves outcomes for most or all patients. While gene therapy has elicited considerable excitement, the need for bone marrow ablation and the high cost preclude broad application of this approach for the foreseeable future, while millions worldwide would benefit from new, affordable, and easily accessible therapies. Thus, new small

molecule approaches are desperately needed, but the pipeline for identification and validation of new therapies is extremely limited.

All the most promising therapeutic approaches for SCD proposed to date, gene therapy, fetal hemoglobin (HbF) induction, and hemoglobin oxygen affinity modulation, act by reducing the amount of polymer in sickle red blood cells (RBCs). However, the only FDA-approved drug targeting sickle hemoglobin (HbS) polymerization, voxelotor, has not yet shown broad efficacy and questions remain about its pharmacodynamics and long-term effects.<sup>7–10</sup> Moreover, only a handful of small molecule therapies have ever been proposed to target HbS polymerization directly. A major reason for this dearth of therapies is the lack of high throughput screening (HTS) assays with which to identify molecules that can inhibit HbS polymerization. One challenge in developing HTS-compatible assays for HbS polymerization is that nucleation of polymer may begin in a wide temporal window, and the

Received: May 26, 2022

Revised: July 22, 2022

Published: August 9, 2022



polymer growth is extremely rapid upon nucleation.<sup>11–16</sup> Thus, measuring polymer growth kinetics in parallel conditions in 96-, 384-, or 1536-well plates is virtually impossible. The result is that, to our knowledge, no compounds that target HbS polymerization have been developed through traditional screening approaches that are the workhorse of pharmaceutical development.

We speculated that a HTS strategy could be engineered to monitor whether small molecules can prevent the formation of prenucleation oligomers that form in dilute HbS solutions under hypoxic conditions. Prenucleating oligomers of deoxy-HbS have been previously observed at concentrations relevant to nucleation and polymerization ( $\sim 1$  mM),<sup>17,18</sup> but here we show that these oligomers can be measured at orders of magnitude lower concentrations at room temperature, making HTS feasible. Based on this novel observation, we developed a HTS-compatible assay using high-sensitivity lifetime FRET, and we demonstrated that this assay is sensitive to compounds that inhibit deoxy-HbS polymerization. We also report the results of a pilot small-molecule screen in which we discovered several novel inhibitors of HbS oligomerization. Finally, we report the validation of those novel inhibitors in solution and in whole blood from sickle patients using *ex vivo* microfluidic measurements of blood flow.

## EXPERIMENTAL SECTION

**Preparation and Characterization of Nonfibrillar Oligomers.** Oligomerization of deoxy-HbS at subnucleating concentrations was measured using dynamic light scattering (DLS). Brookhaven's 90 plus particle size analyzer equipped with a 633 nm He–Ne laser was used to measure the effective diameter of HbS. This laser produces a vertically polarized beam with a wavelength of 632.8 nm. Effective diameter was measured at a scattering angle of 90°. For this assay, HbS (2 mg/mL) was dissolved in filtered PBS and then centrifuged at 13000g for 5–10 min at 4 °C to remove the debris. After centrifugation, HbS supernatant was recovered. To make dust-free samples for DLS experiments, all samples were passed through a 0.2  $\mu$ m filter. Protein concentration was measured spectrophotometrically using Beer's law. Next, HbS (25 mM) sample was incubated with hit compounds at room temperature for 2 h. Next, HbS was vacuum degassed for 5–10 min. Then, oligomerization of deoxy-HbS was measured using DLS. Stability of nonfibrillar oligomers was determined by taking the DLS readings every minute at 25 °C for 2 h. All DLS data reported here are taken with unlabeled protein.

**Development of HTS Platform for Identification of Small Molecules That Inhibit *In Vitro* HbS Nucleation.** Sickle hemoglobin (HbS) (Sigma) was labeled with either fluorescent donor (rhodamine red) or acceptor (Cy5) dyes (Thermo Fisher Scientific) via a cysteine thiol group. For labeling, lyophilized HbS (10 mg/mL) was dissolved in PBS (Sigma) and then centrifuged at 13000g for 5 min at 4 °C to remove the debris. After centrifugation, the protein sample was incubated with tris(2-carboxyethyl)phosphine (TCEP, 0.5–1 mM) for 20 min at room temperature to reduce the cysteine side chain. This protein mixture was incubated with 1.5 mM dye (dissolved in DMSO or water) for 2 h in the dark at room temperature or overnight at 4 °C. Unreacted free dye was removed by dialysis against PBS. The degree of labeling was calculated by comparing the absorption of the fluorophore conjugated hemoglobin at 280 nm to the absorbance of the dye at its maximum wavelength. The dye concentration was measured by absorbance, using extinction coefficients of 250 000 M<sup>-1</sup> cm<sup>-1</sup> for Cy5 conjugates and 88000 M<sup>-1</sup> cm<sup>-1</sup> for rhodamine red conjugates.

**High-Throughput Screening of LOPAC Library to Identify Compounds That Inhibit HbS Oligomerization under Deoxygenated Conditions.** The LOPAC compounds (Thermo Fisher Scientific) were received in 96-well plates. Assay plates were prepared

by transferring 5 nL of the 10 mM compound stocks or DMSO from the source plates to 1536-well black polypropylene plates (Greiner), using an Echo 550 acoustic dispenser (Labcyte). During screening, donor sample (HbS/rhodamine red) was mixed with acceptor (HbS/Cy5) at 1:5 ratios. Then protein samples were dispensed (5  $\mu$ L, 25  $\mu$ M) by a Multidrop Combi Reagent Dispenser (Thermo Fisher Scientific) into the 1536-well assay plates containing the compounds and incubated at room temperature for 2 h. After incubation, protein samples were degassed for 10–15 min using vacuum argon degassing method. Lifetime measurements were taken with the fluorescence lifetime plate reader (Fluorescence Innovations, Inc.).

**Fluorescence Data Acquisition.** We tested the functionality of the HbS FRET pair by measuring lifetimes of oxy- and deoxy-HbA and -HbS using a fluorescence lifetime plate reader (Figure S2A). Lifetimes are reciprocally related to FRET, so a decrease in lifetime corresponds to an increase in FRET. Donor fluorescence was excited with a 532 nm laser (Teem Photonics SNG-20F-100, Meylan, France), delivering pulses of  $\sim 0.3$   $\mu$ J energy at a 20 kHz repetition rate, and emission was filtered with 546 nm long pass and 586/20 nm band-pass filters. These filters were selected to exclude acceptor fluorescence, as only the lifetime of the donor fluorescent protein is required to calculate FRET (eq 1). The photomultiplier tube (PMT) voltage was adjusted so that the peak signals of the instrument response function (IRF) and FRET biosensor were similar.

**High Throughput Screening Data Analysis.** Time resolved fluorescence waveforms for each well were fitted with single-exponential decays using least-squares minimization global analysis software.<sup>19</sup> FRET efficiency ( $E$ ) was determined as the fractional decrease of donor lifetime ( $\tau_D$ ), due to the presence of acceptor fluorophore ( $\tau_{DA}$ ) using eq 1:

$$E = 1 - \left( \frac{\tau_{DA}}{\tau_D} \right) \quad (1)$$

Assay quality was determined based on controls (phenylalanine as a positive control and DMSO as negative control) on each plate, as indicated by the  $Z'$  factor.<sup>20</sup>

$$Z' = 1 - \frac{3(\sigma_p + \sigma_n)}{|\mu_p - \mu_n|} \quad (2)$$

where  $\sigma_p$  and  $\sigma_n$  are the standard deviations (SDs) and  $\mu_p$  and  $\mu_n$  are the means of the positive and negative controls, respectively.

**FRET Dose–Response Assay.** The hit compounds, chlormezanone, gabazine, and phosphoramidon disodium, were purchased from Sigma. These drug compounds were dissolved in DMSO to make 20 mM stock solution. Hits were screened at seven different concentrations. Protein samples were dispensed into the 384-well assay plates and incubated with hit compounds at room temperature for 2 h. After incubation, protein samples were degassed for 10 min using vacuum argon degassing method. Lifetime measurements were taken by the fluorescence lifetime plate reader (Fluorescence Innovations, Inc.).

**Polymerization of Deoxy-HbS in High Phosphate Buffer.** Effect of hit compounds on polymerization of deoxy-HbS in high potassium phosphate buffer was monitored using Spectramax i3X. High concentration phosphate buffer (1.895 M potassium phosphate (KPi)) was made by dissolving solid monobasic and dibasic potassium phosphate in deionized water with final pH 7.3. Purified HbS was concentrated in high phosphate buffer by buffer exchange using spin concentrators at 4 °C. On the day of experiment, the temperature of the Spectramax i3X was set to 37 °C. Next, plastic 1 mL UV cuvettes were placed on ice, and 950  $\mu$ L of 1% *m*-maleimidobenzoyl-*N*-hydroxysuccinimide ester (MBS) in 1.895 KPi was quickly pipetted into each cuvette. Then, 50  $\mu$ L of HbS (24 mg/mL, final concentration 1.2 mg/mL) was added to the cuvette, the contents were mixed, and the cuvette was placed into the Spectramax. The cuvette reached the set temperature in about 3 min, and the HbS was completely converted into deoxy-HbS in this time. The delay time for 1.2 mg/mL HbS is around 470 s, and the midpoint is around

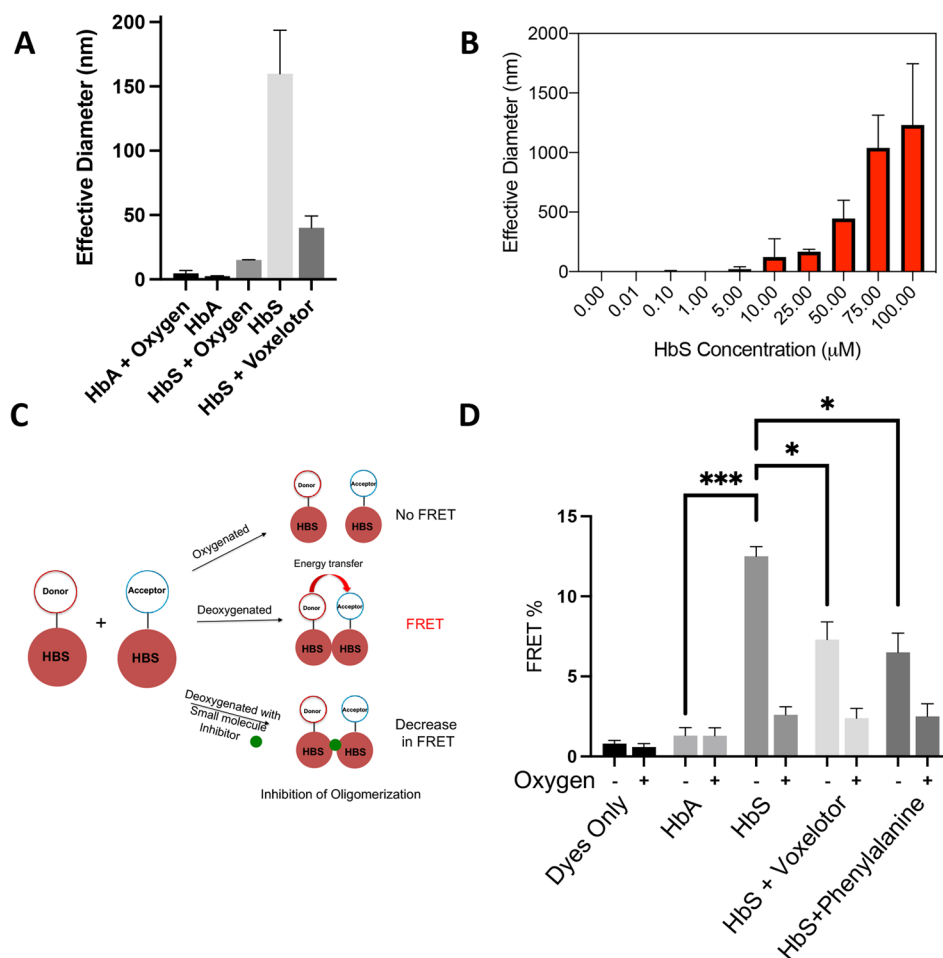


**Figure 1.** Direct measurement of prefibrillar HbS oligomers by DLS and FRET. (A) Confirmation of oligomerization via DLS. Purified HbA or HbS (25  $\mu\text{M}$ ) was vacuum degassed with argon for 5 min, and then DLS measurements were taken at room temperature. (B) HbS oligomer size versus concentration. Purified HbS (0.01–100  $\mu\text{M}$ ) was degassed with argon for 5 min, and then DLS measurements were taken at room temperature. (C) Schematic of TR-FRET scheme. Time-resolved FRET can be used to probe association of deoxy-HbS monomers in solution and to discover small molecules that disrupt these assemblies. (D) FRET efficiency of fluorescent dyes, fluorescently labeled HbA and HbS samples under deoxygenated and oxygenated conditions. FRET efficiency of HbS sample was increased under deoxygenated conditions, demonstrating that the signal is specific to association of HbS in the absence of fibers. Voxelotor and phenylalanine, which are known to inhibit polymerization, reduced FRET efficiency of HbS under deoxygenated conditions. All DLS data are reported as the effective diameter of the mean assembly size. Hypothesis testing was performed using parametric ANOVA with Dunnett's multiple comparison testing. \* $p$ -value < 0.05; \*\* $p$ -value < 0.01; \*\*\* $p$ -value < 0.001.

520 s. Next, a 700 nm absorbance reading was taken every 3 s. Growth curves were normalized by setting the initial linear part of the curve, typically from 500 to 1500 s, to baseline at zero and then normalizing the end of the curves (which would be completely fibrillized) to 100% fibrillized. Lines were fit to the linear part of the growth curves, and the slopes were taken as the growth rate and compared between conditions.

**Blood Sample Collection and Preparation for Microfluidic Assays.** Sick cell patient blood samples were collected under protocols approved by the Institutional Review Boards at Children's Minnesota Hospital, the University of Minnesota Medical Center, and the University of Minnesota. Patient blood samples were collected into sodium citrate Vacutainer tubes and stored at 4  $^{\circ}\text{C}$ . The samples were prepared for the microfluidic experiments by washing twice with Dulbecco's phosphate buffered saline (DPBS) after centrifugation for 5 min at 400g. Packed red blood cells were then isolated by centrifuging the washed samples for 10 min at 400g and removing all remaining DPBS. The packed red blood cells were added to fresh DPBS to achieve a target hematocrit of 25%. Each compound of interest was added to the sample to reach a target concentration of 500  $\mu\text{M}$ , and samples were incubated at 37  $^{\circ}\text{C}$  for 1 h before being

run on the microfluidic device. The compounds were dissolved in DMSO at a concentration of 100 mM and stored at  $-20^{\circ}\text{C}$  or  $-80^{\circ}\text{C}$  prior to use.

**Microfluidic Setup and Experimental Protocol.** A previously described<sup>21–23</sup> polydimethylsiloxane (PDMS) microfluidic device replicating the geometry of the postcapillary venules was used to study blood rheological behavior. Figure S5 shows the device layout with the inputs and outputs for each of the three layers. The microfluidic channels were primed by flowing a 2% bovine serum albumin (BSA) in DPBS solution through the device to passivate the PDMS surface. Blood was then added to the inlet port and flowed through the device under a constant driving pressure to achieve an initial velocity of 700  $\mu\text{m/s}$  (PCD-15PSIG, Alicat Scientific). At the bifurcation, blood was diverted to two 15  $\mu\text{m} \times 15 \mu\text{m}$  square channels, a bypass channel and an experimental channel. Separate gas inlets supplied oxygen to each of the two blood channels independently via diffusion from the overlaid gas layer. The bypass channel was supplied with air and maintained under normoxic conditions. In the experimental channel, a gas mixing system was used to control the oxygen level on the device, and the level was recorded with a fiber optic oxygen sensor ((NeoFox-GT, Ocean Optics,

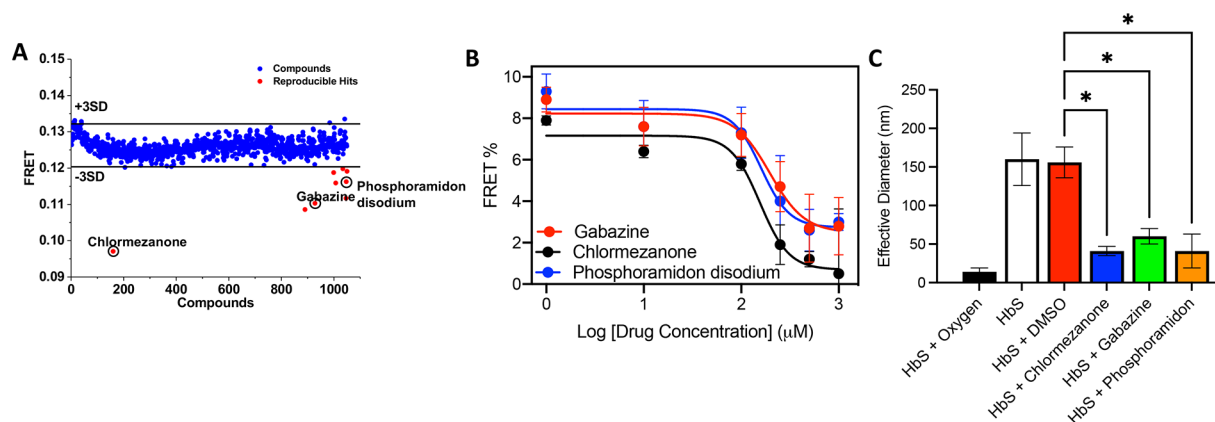


**Figure 2.** Lifetime FRET HTS. (A) Pilot screening with LOPAC library. Compounds that reduced the FRET efficiency below 3SD (black line) were selected for further characterization. Nine hit compounds with reproducible FRET change were identified from the pilot screens (red). (B) Dose response curves of three HbS hit compounds (panel A, red circles). Fluorescently labeled HbS samples were dispensed into a 1536-well plate and treated separately with DMSO or the three hit compounds, chlormezanone, gabazine, and phosphoramidon disodium, in a dose-dependent manner from 0.1 to 1000  $\mu\text{M}$  for 2 h at room temperature and then vacuum degassed for 10 min, and then donor lifetimes were measured using a fluorescence plate reader. (C) Effective diameter of HbS in the presence and absence of hit compounds from DLS measured at 90°. HbS samples (25  $\mu\text{M}$ ) were incubated separately with hit compounds (100  $\mu\text{M}$ ) or DMSO only for 2 h at room temperature and degassed with argon for 5 min, and then DLS measurements were taken at room temperature. Hypothesis testing was performed using parametric ANOVA with Dunnett's multiple comparison testing. \* $p$ -value < 0.05; \*\* $p$ -value < 0.01; \*\*\* $p$ -value < 0.001.

Dunedin, FL). Air (21%  $\text{O}_2$ ) was supplied to the experimental region of the device for 3 min, followed by 5 min of hypoxia. The degree of hypoxia was increased with each successive cycle in 2%  $\text{O}_2$  increments (Figure S6A). A high-speed camera continuously collected four-frame bursts of images of the channel at 40 $\times$  magnification on a Zeiss Axio Vert.A1 microscope (Carl Zeiss, Oberkochen, Germany). The bursts of images were analyzed frame-by-frame in real time using the Kanade–Lucas–Tomasi (KLT) feature tracking algorithm in Matlab (Mathworks, Natick, MA) to determine the average velocity of the blood through the channel (Figure 3A).

**Microfluidic Measurement of RBC Oxygen Saturation.** The quantitative absorption cytometry assay described previously<sup>24,25</sup> takes images of single red blood cells (RBCs) under alternating 410 and 430 nm LEDs. Due to the unique absorption spectra of oxy- and deoxyhemoglobin, the transmitted light at 410 and 430 nm permits calculation of the single cell saturation. The cells are perfused through a microfluidic device with oxygen control that permits measurement of the oxygen saturation of a population of RBCs under defined oxygen tension. The polydimethylsiloxane (PDMS) microfluidic device for this assay comprises two layers, a gas layer and a blood layer, bonded to a glass coverslip. These two layers are separated by 100  $\mu\text{m}$  of PDMS. The gas layer allows for precise control of oxygen tension that will diffuse to the blood layer; the blood layer contains a 30 mm diffusion section to allow red blood cells to reach steady state saturation and a 5 mm observation section for imaging RBCs.

To prepare RBCs for measurement, blood samples were washed and resuspended in 10% w/v BSA in PBS, and 0.5  $\mu\text{L}$  of 100 mM therapeutic agent in DMSO was added to the sample. The sample was then incubated on a shaker plate at 37  $^\circ\text{C}$  for 1 h. After incubation, samples were washed again, and 10  $\mu\text{L}$  of packed red blood cells was added to a solution of 288  $\mu\text{L}$  of 25% human serum albumin (HSA) solution (Gemini Bio).

In this assay, we prepared samples identically to the preparation for blood flow by incubating with drug at 25% hematocrit, and then we diluted the samples to 1% hematocrit with 500  $\mu\text{M}$  drug in the dilution buffer. The use of drug in the running buffer after dilution of the RBCs was done to ensure that we did not dilute any drug effects relative to the whole blood studies. This preparation resulted in higher modification (~100%) of hemoglobin by voxelator than in the whole blood studies, yielding a large shift in P50 (Figure S7A).

## RESULTS AND DISCUSSION

**Prefibrillar HbS Oligomers Can Be Measured at Subnucleating Concentrations.** To test the hypothesis that deoxy-HbS forms stable oligomers at subnucleating concentrations, we measured HbS solutions by DLS and found that HbS (but not HbA) formed oligomers larger than the tetrameric protein under fully anoxic conditions (Figure 1A).

We also found that deoxy-HbS forms oligomers that vary in size with concentration (Figure 1B). To test the hypothesis that these oligomers are sensitive to drugs that inhibit polymer formation, we measured them in the presence of voxelator (a compound that increases hemoglobin oxygen binding affinity), which dramatically reduced the mean oligomer size (Figure 1A). We also found that the oligomers were temporally stable (Figure S1A) and that DMSO did not affect the oligomer size (Figure S1B), two essential points that make HTS feasible.

As an orthogonal modality to DLS, we developed a fluorescence lifetime (FLT) FRET assay (Figure 1C) to measure deoxy-HbS oligomers. As shown in Figure 1D, measurements of deoxy-HbS showed a substantial increase in FRET efficiency (measured as a decrease in the donor FLT in the presence of the acceptor compared with the donor only, Figure S2A), which corresponds to association of the deoxy-HbS molecules. By contrast, oxy- and deoxy-HbA and oxy-HbS showed no significant increase in FRET efficiency in the presence of the acceptor. We tested the effect of voxelator and phenylalanine on the oligomerization of deoxy-HbS,<sup>2,26,27</sup> and both molecules decreased the FRET efficiency (Figure 1D), demonstrating that the FRET-based assay is sensitive to compounds that are known to inhibit deoxy-HbS polymerization.

**High-Throughput FLT FRET Reveals Novel Inhibitors of HbS Oligomerization.** Using the lifetime FRET assay, we performed HTS of the LOPAC library (1284 compounds) as a pilot to determine if the method can identify small molecules that inhibit deoxy-HbS oligomerization. The screen was enabled by a high-throughput FLT plate reader technology.<sup>28</sup>

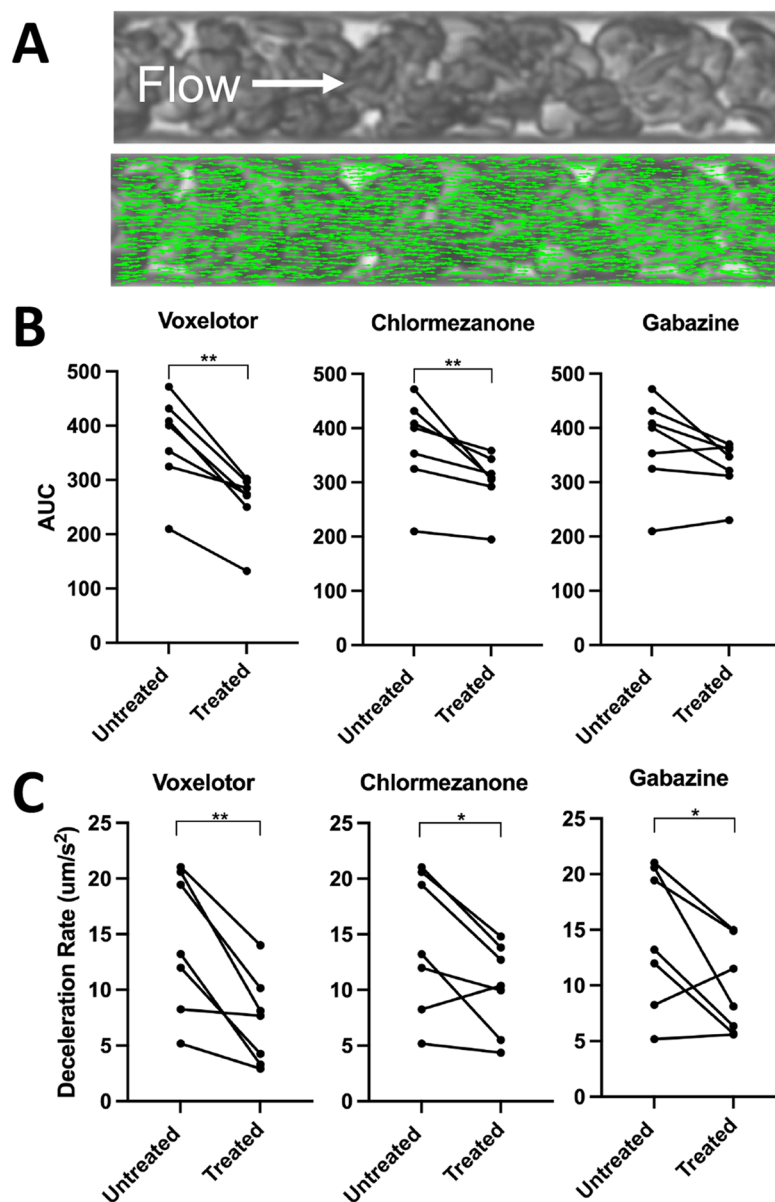


**Figure 3.** Hit compounds reduce hypoxia-induced blood flow impairment. We treated RBC suspensions at 25% hematocrit from 7 individuals with SCD (genotype HbSS) with 500  $\mu\text{M}$  of our hit compounds or voxelotor (positive control) and quantified the flow in our microfluidic platform under well-defined oxygen tensions. (A) Representative image of blood flowing in microfluidic device with overlay of green arrows representing the velocities of features between frames using the Kanade–Lucas–Tomasi algorithm. (B) Area under velocity response curve (AUC) comparison among treated samples compared to the vehicle control. (C) Deceleration rate comparison among treated samples compared to the vehicle control. All statistics were performed using a one-tailed Wilcoxon signed rank test,  $\alpha = 0.05$ , \* $p$ -value < 0.05, \*\* $p$ -value < 0.01.

FRET efficiencies from all compounds that were not fluorescent were averaged from three independent screens (Figure 2A). We identified nine compounds that were at least  $3\sigma$  from the mean of all compounds, based on a Gaussian fit of the histograms (Figure S2B). Four of these hit compounds reduced the FRET efficiency by more than 20% (Figure 2A, red circles), with chlormezanone having by far the largest effect. We also checked if controls and hit compounds acted as a quencher (thereby artificially decreasing the FRET signal without preventing oligomerization) by testing their effect on donor only lifetime. If compounds are fluorescence quenchers, we would see a change in donor only lifetime when compared with DMSO control. We did not observe a significant change in donor only lifetimes in the presence of compounds (Figure

S2C). These results further confirm that decrease in FRET is due to inhibition of deoxy-HbS oligomerization. A subset of hit compounds (chlormezanone, gabazine, and phosphoramidon disodium) were evaluated using dose response with FRET (Figure 2B), and all three compounds decreased FRET efficiency in a dose-dependent manner, again with chlormezanone showing the biggest effect at an  $\text{IC}_{50} > 100 \mu\text{M}$ . We also measured the size of deoxy-HbS oligomers using DLS in the presence and absence of hit compounds (Figure 2C) and found that all three compounds significantly decreased the oligomer size relative to control (and to the same extent as voxelotor). We tested the ability of chlormezanone and gabazine to inhibit polymerization and found a modest, dose-responsive decrease in the rate of fibril growth with

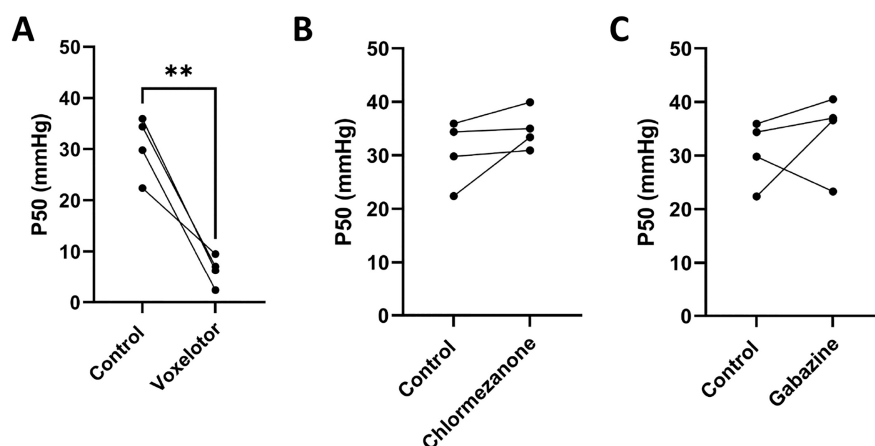


**Figure 4.** Hit compounds do not increase hemoglobin oxygen binding affinity. Measurement of hemoglobin oxygen saturation in RBCs from 4 healthy donors (genotype HbAA). RBCs at 25% hematocrit were incubated with 500  $\mu$ M voxelotor, chlormezanone, or gabazine or DMSO (control) for 1 h at 37  $^{\circ}$ C and then diluted to 1% hematocrit with drug. Voxelotor significantly decreased the P50 of the treated RBCs ( $p = 0.027$ ). Chlormezanone and gabazine resulted in no significant ( $p > 0.05$ ) change in P50 relative to control.

chlormezanone (20% at 100  $\mu$ M, Figure S3), with a less compelling result for gabazine. Unlike voxelotor,<sup>2</sup> these initial hit compounds do not eliminate fibril growth altogether. Finally, we used NMR to directly confirm binding of chlormezanone to HbS (Figure S4). Together these data suggest that our FLT screening method can reveal small molecules that bind to HbS and inhibit deoxy-HbS oligomerization in solution but that larger library screens will be needed to identify compounds that potentially inhibit polymerization at physiological HbS concentrations.

**Hit Compounds Reduce Oxygen-Dependent Blood Flow Impairment.** We evaluated whether the hits could reduce hypoxia-induced impairment of sickle blood flow using previously published microfluidic devices (Figure S5, Figure 3A).<sup>23,29</sup> We treated RBCs from 7 individuals with SCD (genotype HbSS) with 500  $\mu$ M chlormezanone, gabazine, or voxelotor (positive control) and quantified the oxygen-dependent flow in our microfluidic platform (Figure S6A,B). The 500  $\mu$ M dose represents the maximum whole blood concentration observed for the FDA-approved dosage of voxelotor and corresponds to 35–45% modification of the hemoglobin at 25% hematocrit (assuming complete RBC partitioning and 30–36 g/dL intracellular hemoglobin concentration).<sup>30</sup>

We quantified the area under the velocity response curve (AUC, Figure S6C) and the rate of deceleration (Figure S6D) for each treatment condition. As shown in Figure 3B, chlormezanone and voxelotor significantly reduced the mean AUC ( $p = 0.0078$ ), relative to control, while samples treated with gabazine showed an insignificant trend toward reduced AUC ( $p = 0.0547$ ). Chlormezanone, gabazine, and voxelotor all significantly reduced the deceleration rate of blood during deoxygenation (Figure 3C,  $p = 0.0391$  for chlormezanone and gabazine,  $p = 0.0078$  for voxelotor).

**Hit Compounds Do Not Increase Hemoglobin Oxygen Affinity.** A major mechanistic question is whether compounds discovered with our screening method inhibit oligomerization by increasing hemoglobin oxygen binding affinity, similar to voxelotor, or by some other mechanism.

Using a previously described microfluidic platform,<sup>24,25</sup> we quantified the oxygen binding curves of RBCs from 4 healthy donors (genotype HbAA) with and without incubation with

chlormezanone, gabazine, or voxelotor (positive control) at 500  $\mu$ M. As expected, voxelotor significantly ( $p < 0.05$ ) decreases P50, indicating an increase in oxygen binding affinity (Figure 4A). However, neither chlormezanone nor gabazine significantly shifted P50 (Figure 4B,C), and for most of the samples tested, the trend was that these compounds slightly increased P50, strongly suggesting that they do not act by increasing oxygen binding affinity.

The HTS strategy presented here, which uses high-sensitivity lifetime FRET (Figures 1C,D) to monitor temporally stable prefibrillar deoxy-HbS oligomers (confirmed with DLS, Figure S1B), circumvents the challenges of highly parallelized quantification of deoxy-HbS polymerization such as high protein concentration and stochastic nucleation events. The use of FLT detection is a major advantage of our assay because it increases the precision of FRET-based screening by a factor of 30 compared with conventional fluorescence intensity detection.<sup>28</sup> Additionally, our labeling methodology overcomes the technical challenge that traditional FRET probe emission peaks overlap with hemoglobin absorption peaks. The result is an excellent HTS assay with  $Z' = 0.65$  and the possibility of further optimization.<sup>20</sup> While we do not know the structure of the deoxy-HbS oligomers measured in these studies, the sensitivity of the oligomers to phenylalanine and voxelotor strongly suggests that the oligomers share at least some critical bonds with the polymer, making them a suitable target for drug discovery. Moreover, because these are pre-nucleation oligomers, drugs that disrupt them are likely to inhibit or delay nucleation, which is the goal of most antisickling therapies.<sup>31</sup>

We have shown that this breakthrough HTS assay is sensitive to compounds that inhibit deoxy-HbS polymerization by increasing oxygen binding affinity (voxelotor, Figure 1D). With voxelotor clinically approved and a new oxygen affinity modulator in clinical trials,<sup>32,33</sup> the need for finding new molecules of this type may be limited. However, our assay is also sensitive to small molecules that inhibit deoxy-HbS oligomerization independent of oxygen affinity, and we have found several such compounds here although their mechanism of action remains unknown. There is little structural similarity among gabazine, chlormezanone, and voxelotor. This is consistent with chlormezanone and gabazine not shifting

oxygen binding affinity and suggests that they are noncovalent binders. Chlormezanone and gabazine have unique core structures from each other and, most likely, a unique binding mode to HbS. We can only speculate about their mechanism of action, but they might act via two possible mechanisms: (1) in the presence of hit compounds, hemoglobin might adopt a slightly different conformation where the acceptor hydrophobic pocket becomes inaccessible to  $\beta 6$ -valine to oligomerize or (2) hit compounds might be competing with  $\beta 6$ -valine for interaction with the acceptor hydrophobic pocket on the surface of an adjacent Hb molecule. Regardless of the mechanism, the low potency of chlormezanone and gabazine in the fibrillization assay suggest that they are likely not strong lead molecules. Additionally, these compounds have known adverse effects (chlormezanone<sup>34</sup>) and off-target effects (gabazine<sup>35,36</sup>). In fact, it would be highly unusual to find a high-potency lead in such a small library, and thus this initial study was intended as proof-of-principle for this new approach. To realize the promise of this novel mechanism as a clinically effective approach will depend on the existence of a high-specificity binding site for this class of compounds, which we have not proven here. The hit rate in our pilot screen offers hope that such compounds could be found by screening large libraries and using medicinal chemistry.

The development of this HTS platform comes at a critical time in the development of new therapies for SCD. The World Health Organization and United Nations recognize SCD as a global health issue.<sup>37</sup> According to the Centers for Disease Control, SCD affects over 100 000 individuals in the US, primarily in Black communities, worsening the health disparity among minority populations.<sup>38</sup> Furthermore, in resource-poor nations fewer than 50% of children with SCD survive beyond 5 years of age.<sup>39,40</sup> Hence, there is a deep need to accelerate therapeutic discovery. There is also a growing recognition that gene therapy, while potentially curative, is too costly and complex to become a broadly applicable strategy for the millions with SCD worldwide. Thus, the tools for developing new small molecule therapies must be expanded and enhanced. It is worth noting that of the currently approved therapies, only voxelotor would have been discovered using our screening approach. While HbS polymerization is the core molecular mechanism of the disease, there is also room for assays to discover therapies that target other elements of the pathophysiology. In the context of inhibiting polymerization, we know of at least two other efforts to screen drugs for SCD, including recent work by Pfizer that resulted in a drug now in clinical trials<sup>32</sup> and work by Bill Eaton and colleagues at NIH that has found promising hits using a cell-based HTS assay (personal communication, unpublished as of the submission of this manuscript).<sup>41,42</sup> After seven decades, traditional large-scale drug discovery campaigns for SCD are now underway and promise to revolutionize treatment options for this terrible disease.

## CONCLUSIONS

In this study, we present the first observation of stable deoxy-HbS oligomers at subnucleating concentrations. Leveraging the existence of these species, we developed a FLT FRET-based HTS assay for identifying small molecules that inhibit oligomerization of sickle hemoglobin. We showed that this assay is sensitive to small molecules that inhibit oligomerization and polymerization of HbS under deoxygenated conditions. We also reported the results of a pilot small-

molecule screen in which we identified several novel inhibitors of HbS oligomerization. Finally, using *ex vivo* microfluidic measurements, we validated that 2 of our top hits were able to inhibit HbS polymerization in RBC and decrease impairment of sickle blood flow under hypoxic conditions. This screening approach opens the door to large scale HTS screening for small molecules that could reduce the morbidity and mortality in SCD and improve the lives of millions worldwide.

## ASSOCIATED CONTENT

### Supporting Information

The Supporting Information is available free of charge at <https://pubs.acs.org/doi/10.1021/acs.biomac.2c00671>.

DLS characterization of HbS oligomers, lifetime FRET, fibrillization assay, chlormezanone binding confirmed by NMR, schematic of microfluidic device for measuring sickle blood flow, and quantification of sickle blood flow (PDF)

## AUTHOR INFORMATION

### Corresponding Authors

**Jonathan N. Sachs** – Department of Biomedical Engineering, University of Minnesota, Minneapolis, Minnesota 55455, United States; [orcid.org/0000-0003-1403-5960](https://orcid.org/0000-0003-1403-5960); Email: [jnsachs@umn.edu](mailto:jnsachs@umn.edu)

**David K. Wood** – Department of Biomedical Engineering, University of Minnesota, Minneapolis, Minnesota 55455, United States; [orcid.org/0000-0001-5225-2144](https://orcid.org/0000-0001-5225-2144); Email: [dkwood@umn.edu](mailto:dkwood@umn.edu)

### Authors

**Nagamani Vunnam** – Department of Biomedical Engineering, University of Minnesota, Minneapolis, Minnesota 55455, United States

**Scott Hansen** – Department of Biomedical Engineering, University of Minnesota, Minneapolis, Minnesota 55455, United States

**Dillon C. Williams** – Department of Biomedical Engineering, University of Minnesota, Minneapolis, Minnesota 55455, United States

**MaryJane Olivia Been** – Department of Biomedical Engineering, University of Minnesota, Minneapolis, Minnesota 55455, United States

**Chih Hung Lo** – Department of Biomedical Engineering, University of Minnesota, Minneapolis, Minnesota 55455, United States

**Anil K. Pandey** – Department of Biomedical Engineering, University of Minnesota, Minneapolis, Minnesota 55455, United States

**Carolyn N. Paulson** – Department of Biomedical Engineering, University of Minnesota, Minneapolis, Minnesota 55455, United States; [orcid.org/0000-0001-8564-7345](https://orcid.org/0000-0001-8564-7345)

**John A. Rohde** – Department of Biochemistry, Molecular Biology, and Biophysics, University of Minnesota, Minneapolis, Minnesota 55455, United States

**David D. Thomas** – Department of Biochemistry, Molecular Biology, and Biophysics, University of Minnesota, Minneapolis, Minnesota 55455, United States

Complete contact information is available at: <https://pubs.acs.org/10.1021/acs.biomac.2c00671>

## Author Contributions

Conceptualization: D.D.T., J.N.S., D.K.W. Methodology: N.V., S.H., C.H.L., C.P., A.P., J.R., D.D.T., J.N.S., D.K.W. Investigation: N.V., S.H., M.J.B., C.H.L., C.P., A.P. Visualization: N.V., S.H., C.H.L., C.P., D.K.W. Supervision: J.N.S., D.K.W. Writing—original draft: N.V., S.H., J.N.S., D.K.W. Writing—review and editing: N.V., S.H., C.P., J.R., D.D.T., J.N.S., D.K.W.

## Notes

The authors declare the following competing financial interest(s): D.D.T. holds equity in and serves as President of Photonic Pharma LLC. This relationship has been reviewed and managed by the University of Minnesota. Photonic Pharma had no role in this study.

## ACKNOWLEDGMENTS

We thank the patients at Children's Hospital and Clinics of Minnesota for their generous blood donations and the sickle care team, including Dr. Steve Nelson, Ashley Kinsella, Pauline Mitby, Ali Koste, Rachel Hinsch, and Emily Olson for blood sample collection. We acknowledge funding under Grants R01HL132906 (D.K.W.), R21HL152313 (J.N.S., D.K.W.), and R35GM131814 (J.N.S.). Portions of this work were conducted in the Minnesota Nano Center, which is supported by the National Science Foundation through the National Nanotechnology Coordinated Infrastructure (NNCI) under Award Number ECCS-2025124.

## REFERENCES

- (1) Dufu, K.; Patel, M.; Oksenberg, D.; Cabrales, P. GBT440 improves red blood cell deformability and reduces viscosity of sickle cell blood under deoxygenated conditions. *Clin Hemorheol Microcirc* **2018**, *70* (1), 95–105.
- (2) Oksenberg, D.; Dufu, K.; Patel, M. P.; Chuang, C.; Li, Z.; Xu, Q.; Silva-Garcia, A.; Zhou, C.; Hutchaleelaha, A.; Patskovska, L.; Patskovsky, Y.; Almo, S. C.; Sinha, U.; Metcalf, B. W.; Archer, D. R. GBT440 increases haemoglobin oxygen affinity, reduces sickling and prolongs RBC half-life in a murine model of sickle cell disease. *Br. J. Haematol.* **2016**, *175* (1), 141–53.
- (3) Jafri, F.; Seong, G.; Jang, T.; Cimpeanu, E.; Poplawska, M.; Dutta, D.; Lim, S. H. L-glutamine for sickle cell disease: more than reducing redox. *Ann. Hematol.* **2022**, *101* (8), 1645–1654.
- (4) Ataga, K. I.; Kutlar, A.; Kanter, J.; Liles, D.; Cancado, R.; Friedrisch, J.; Guthrie, T. H.; Knight-Madden, J.; Alvarez, O. A.; Gordeuk, V. R.; Gualandro, S.; Colella, M. P.; Smith, W. R.; Rollins, S. A.; Stocker, J. W.; Rother, R. P. Crizanlizumab for the Prevention of Pain Crises in Sickle Cell Disease. *N Engl J. Med.* **2017**, *376* (5), 429–439.
- (5) Charache, S.; Terrin, M. L.; Moore, R. D.; Dover, G. J.; Barton, F. B.; Eckert, S. V.; McMahon, R. P.; Bonds, D. R. Effect of hydroxyurea on the frequency of painful crises in sickle cell anemia. Investigators of the Multicenter Study of Hydroxyurea in Sickle Cell Anemia. *N Engl J. Med.* **1995**, *332* (20), 1317–22.
- (6) Cokic, V. P.; Smith, R. D.; Beleslin-Cokic, B. B.; Njoroge, J. M.; Miller, J. L.; Gladwin, M. T.; Schechter, A. N. Hydroxyurea induces fetal hemoglobin by the nitric oxide-dependent activation of soluble guanylyl cyclase. *J. Clin Invest.* **2003**, *111* (2), 231–9.
- (7) Han, J.; Saraf, S. L.; Gordeuk, V. R. Systematic Review of Voxelotor: A First-in-Class Sickle Hemoglobin Polymerization Inhibitor for Management of Sickle Cell Disease. *Pharmacotherapy* **2020**, *40* (6), 525–534.
- (8) Hebbel, R. P.; Hedlund, B. E. Sickle hemoglobin oxygen affinity-shifting strategies have unequal cerebrovascular risks. *Am. J. Hematol.* **2018**, *93* (3), 321–325.
- (9) Henry, E. R.; Harper, J.; Glass, K. E.; Metaferia, B.; Louis, J. M.; Eaton, W. A. MWC allosteric model explains unusual hemoglobin-

oxygen binding curves from sickle cell drug binding. *Biophys. J.* **2021**, *120* (12), 2543–2551.

(10) Henry, E. R.; Metaferia, B.; Li, Q.; Harper, J.; Best, R. B.; Glass, K. E.; Cellmer, T.; Dunkelberger, E. B.; Conrey, A.; Thein, S. L.; Bunn, H. F.; Eaton, W. A. Treatment of sickle cell disease by increasing oxygen affinity of hemoglobin. *Blood* **2021**, *138* (13), 1172–1181.

(11) Aprelev, A.; Liu, Z.; Ferrone, F. A. The growth of sickle hemoglobin polymers. *Biophys. J.* **2011**, *101* (4), 885–91.

(12) Castle, B. T.; Odde, D. J.; Wood, D. K. Rapid and inefficient kinetics of sickle hemoglobin fiber growth. *Sci. Adv.* **2019**, *5* (3), eaau1086.

(13) Coletta, M.; Hofrichter, J.; Ferrone, F. A.; Eaton, W. A. Kinetics of sickle haemoglobin polymerization in single red cells. *Nature* **1982**, *300* (5888), 194–7.

(14) Ferrone, F. A.; Hofrichter, J.; Eaton, W. A. Kinetics of sickle hemoglobin polymerization. II. A double nucleation mechanism. *J. Mol. Biol.* **1985**, *183* (4), 611–31.

(15) Ferrone, F. A.; Hofrichter, J.; Eaton, W. A. Kinetics of sickle hemoglobin polymerization. I. Studies using temperature-jump and laser photolysis techniques. *J. Mol. Biol.* **1985**, *183* (4), 591–610.

(16) Ferrone, F. A.; Hofrichter, J.; Sunshine, H. R.; Eaton, W. A. Kinetic studies on photolysis-induced gelation of sickle cell hemoglobin suggest a new mechanism. *Biophys. J.* **1980**, *32* (1), 361–80.

(17) Galkin, O.; Pan, W.; Filobelo, L.; Hirsch, R. E.; Nagel, R. L.; Vekilov, P. G. Two-step mechanism of homogeneous nucleation of sickle cell hemoglobin polymers. *Biophys. J.* **2007**, *93* (3), 902–13.

(18) Wang, Y.; Ferrone, F. A. Dissecting the energies that stabilize sickle hemoglobin polymers. *Biophys. J.* **2013**, *105* (9), 2149–56.

(19) Petersen, K. J.; Peterson, K. C.; Muretta, J. M.; Higgins, S. E.; Gillispie, G. D.; Thomas, D. D. Fluorescence lifetime plate reader: resolution and precision meet high-throughput. *Rev. Sci. Instrum.* **2014**, *85* (11), 113101.

(20) Zhang, J. H.; Chung, T. D.; Oldenburg, K. R. A Simple Statistical Parameter for Use in Evaluation and Validation of High Throughput Screening Assays. *J. Biomol. Screen.* **1999**, *4* (2), 67–73.

(21) Geisness, A. C.; Azul, M.; Williams, D.; Szafraniec, H.; De Souza, D. C.; Higgins, J. M.; Wood, D. K. Ionophore-mediated swelling of erythrocytes as a therapeutic mechanism in sickle cell disease. *Haematologica* **2022**, *107* (6), 1438–1447.

(22) Hansen, S.; Wood, D. K.; Higgins, J. M. 5-(Hydroxymethyl)-furfural restores low-oxygen rheology of sickle trait blood in vitro. *Br. J. Haematol.* **2020**, *188* (6), 985–993.

(23) Valdez, J. M.; Datta, Y. H.; Higgins, J. M.; Wood, D. K. A microfluidic platform for simultaneous quantification of oxygen-dependent viscosity and shear thinning in sickle cell blood. *APL Bioeng.* **2019**, *3* (4), 046102.

(24) Di Caprio, G.; Schonbrun, E.; Goncalves, B. P.; Valdez, J. M.; Wood, D. K.; Higgins, J. M. High-throughput assessment of hemoglobin polymer in single red blood cells from sickle cell patients under controlled oxygen tension. *Proc. Natl. Acad. Sci. U. S. A.* **2019**, *116* (50), 25236–25242.

(25) Di Caprio, G.; Stokes, C.; Higgins, J. M.; Schonbrun, E. Single-cell measurement of red blood cell oxygen affinity. *Proc. Natl. Acad. Sci. U. S. A.* **2015**, *112* (32), 9984–9.

(26) Dufu, K.; Oksenberg, D. GBT440 reverses sickling of sickled red blood cells under hypoxic conditions in vitro. *Hematol. Rep.* **2018**, *10* (2), 7419.

(27) Metcalf, B.; Chuang, C.; Dufu, K.; Patel, M. P.; Silva-Garcia, A.; Johnson, C.; Lu, Q.; Partridge, J. R.; Patskovska, L.; Patskovsky, Y.; Almo, S. C.; Jacobson, M. P.; Hua, L.; Xu, Q.; Gwaltney, S. L., 2nd; Yee, C.; Harris, J.; Morgan, B. P.; James, J.; Xu, D.; Hutchaleelaha, A.; Paulvannan, K.; Oksenberg, D.; Li, Z. Discovery of GBT440, an Orally Bioavailable R-State Stabilizer of Sickle Cell Hemoglobin. *ACS Med. Chem. Lett.* **2017**, *8* (3), 321–326.

(28) Stroik, D. R.; Yuen, S. L.; Janicek, K. A.; Schaaf, T. M.; Li, J.; Ceholski, D. K.; Hajjar, R. J.; Cornea, R. L.; Thomas, D. D. Targeting



protein-protein interactions for therapeutic discovery via FRET-based high-throughput screening in living cells. *Sci. Rep.* **2018**, *8* (1), 12560.

(29) Szafraniec, H. M.; Valdez, J. M.; Iffrig, E.; Lam, W. A.; Higgins, J. M.; Pearce, P.; Wood, D. K. Feature tracking microfluidic analysis reveals differential roles of viscosity and friction in sickle cell blood. *Lab Chip* **2022**, *22* (8), 1565–1575.

(30) Hutchaleelaha, A.; Patel, M.; Washington, C.; Siu, V.; Allen, E.; Oksenberg, D.; Gretler, D. D.; Mant, T.; Lehrer-Graiwer, J. Pharmacokinetics and pharmacodynamics of voxelator (GBT440) in healthy adults and patients with sickle cell disease. *Br. J. Clin. Pharmacol.* **2019**, *85* (6), 1290–1302.

(31) Eaton, W. A.; Bunn, H. F. Treating sickle cell disease by targeting HbS polymerization. *Blood* **2017**, *129* (20), 2719–2726.

(32) Gopalsamy, A.; Aulabaugh, A. E.; Barakat, A.; Beaumont, K. C.; Cabral, S.; Canterbury, D. P.; Casimiro-Garcia, A.; Chang, J. S.; Chen, M. Z.; Choi, C.; Dow, R. L.; Fadeyi, O. O.; Feng, X.; France, S. P.; Howard, R. M.; Janz, J. M.; Jasti, J.; Jasuja, R.; Jones, L. H.; King-Ahmad, A.; Knee, K. M.; Kohrt, J. T.; Limberakis, C.; Liras, S.; Martinez, C. A.; McClure, K. F.; Narayanan, A.; Narula, J.; Novak, J. J.; O'Connell, T. N.; Parikh, M. D.; Piotrowski, D. W.; Plotnikova, O.; Robinson, R. P.; Sahasrabudhe, P. V.; Sharma, R.; Thuma, B. A.; Vasa, D.; Wei, L.; Wenzel, A. Z.; Withka, J. M.; Xiao, J.; Yayla, H. G. PF-07059013: A Noncovalent Modulator of Hemoglobin for Treatment of Sickle Cell Disease. *J. Med. Chem.* **2021**, *64* (1), 326–342.

(33) Knee, K. M.; Jasuja, R.; Barakat, A.; Rao, D.; Wenzel, Z.; Jasti, J.; Novak, J.; Beaumont, K.; Piotrowski, D. W.; Jeffrey, P.; Bulawa, C.; Murphy, J. E.; Janz, J. M. PF-07059013: A non-covalent hemoglobin modulator favorably impacts disease state in a mouse model of sickle cell disease. *Am. J. Hematol* **2021**, *96* (8), E272–E275.

(34) Roupe, G.; Ahlmen, M.; Fagerberg, B.; Suurkula, M. Toxic epidermal necrolysis with extensive mucosal erosions of the gastrointestinal and respiratory tracts. *Int. Arch Allergy Appl. Immunol* **2004**, *80* (2), 145–51.

(35) Behrens, C. J.; van den Boom, L. P.; Heinemann, U. Effects of the GABA(A) receptor antagonists bicuculline and gabazine on stimulus-induced sharp wave-ripple complexes in adult rat hippocampus in vitro. *Eur. J. Neurosci* **2007**, *25* (7), 2170–81.

(36) Iqbal, F.; Ellwood, R.; Mortensen, M.; Smart, T. G.; Baker, J. R. Synthesis and evaluation of highly potent GABA(A) receptor antagonists based on gabazine (SR-95531). *Bioorg. Med. Chem. Lett.* **2011**, *21* (14), 4252–4.

(37) Mburu, J.; Odame, I. Sickle cell disease: Reducing the global disease burden. *Int. J. Lab Hematol* **2019**, *41* (S1), 82–88.

(38) Lee, L.; Smith-Whitley, K.; Banks, S.; Puckrein, G. Reducing Health Care Disparities in Sickle Cell Disease: A Review. *Public Health Rep* **2019**, *134* (6), 599–607.

(39) Uyoga, S.; Macharia, A. W.; Mochamah, G.; Ndila, C. M.; Nyutu, G.; Makale, J.; Tendwa, M.; Nyatichi, E.; Ojal, J.; Otiende, M.; Shebe, M.; Awuondo, K. O.; Mturi, N.; Peshu, N.; Tsoga, B.; Maitland, K.; Scott, J. A. G.; Williams, T. N. The epidemiology of sickle cell disease in children recruited in infancy in Kilifi, Kenya: a prospective cohort study. *Lancet Glob Health* **2019**, *7* (10), e1458–e1466.

(40) Odame, I. Perspective: we need a global solution. *Nature* **2014**, *515* (7526), S10.

(41) Dunkelberger, E. B.; Metaferia, B.; Cellmer, T.; Henry, E. R. Theoretical Simulation of Red Cell Sickling Upon Deoxygenation Based on the Physical Chemistry of Sickle Hemoglobin Fiber Formation. *J. Phys. Chem. B* **2018**, *122* (49), 11579–11590.

(42) Li, Q.; Henry, E. R.; Hofrichter, J.; Smith, J. F.; Cellmer, T.; Dunkelberger, E. B.; Metaferia, B. B.; Jones-Straehle, S.; Boutom, S.; Christoph, G. W.; Wakefield, T. H.; Link, M. E.; Staton, D.; Vass, E. R.; Miller, J. L.; Hsieh, M. M.; Tisdale, J. F.; Eaton, W. A. Kinetic assay shows that increasing red cell volume could be a treatment for sickle cell disease. *Proc. Natl. Acad. Sci. U. S. A.* **2017**, *114* (5), E689–E696.

## NOTE ADDED AFTER ASAP PUBLICATION

This article originally published inadvertently missing an author name and misspelling another author's name. The corrected version published August 17, 2022.